International Journal of Future Generation Communication and Networking
Vol. 13, No. 4, (2020), pp. 207–220

Theoretical Investigation Of The Static Calculation Of A Composite Rolling Chain Drive Roller

Azam Abdumajitovich Mamakhonov,

Doctor of phylosofy in Theory of machines and mechanisms,Docent, Dean of Faculty of Automation and Energetics, Namangan Institute of Engineering and Technology (azamat0783@mail.ru)

Annotation:

The article describes a static and dynamic calculation of the composite roller of the chain drive. The formulas which determine the internal force factors generated in the transversal section of the composite roller under the influence of external loading were obtained. According to the physico-mechanical parameters of the roller, the deformation and internal force factors occurring in the cross section at different values of the elasticity coefficient of the elastic element were determined. In the program MAPLE-17 the required connection graphs are obtained. Under the impact of compressive forces of the teeth of the sprocket, the deformation and internal force factors of the chain drive roller are reduced to 7 ÷ 20 due to the presence of a flexible element.

Keywords: *Chain drive, sprocket, chain, composite roller, elastic element, static, dynamics, deformation, displacement, moment, stress.*

Introduction. In mechanical engineering, chain drive is used as a transmission, load-bearing and fastening, depending on the function of application. The most common type of chains mentioned above are motion-transmitting chains. It is known that the chain drive that transmits motion consists of leading and driven sprockets and an infinite chain surrounding them [1-9].

Among the main disadvantages of existing chain drive structures there is the formation of harmful frictional forces that are generated at the kinematic joints of the chain. Short-term wear of the chain elements will depend on the excess of the leading and driven network cooling. An increase in cooling causes an increase in the amplitude values of the longitudinal and transverse oscillations. This, in turn, leads to a decrease in the efficiency and service life of the transmition, as well as an increase in the amount of noise. As the load and speed increase in the chain drive, an increase in the value of the uneven impact forces in the sprocket-chain connection is observed. As a result, the working elements of chain drive become uneven.

By quenching the shock forces generated at the sprocket teeth and chain joints, the chain drive's working elements can be eroded and the amount of noise can be reduced. This, in turn, leads to a significant increase in chain drive's service life. As a result of scientific research, a new design of the chain drive was developed [10-18].

Materials and methods. The proposed chain drive design consists of a leading and a driven sprocket and an infinite chain enclosing them (Figure 1). The chain drive consists of an inner and outer plate, a roller, a bushing and a composite roller. The composite roller consists of internal and external bushings, respectively, and a flexible element (rubber) bushing located between them. The driven sprocket is designed to be composite and has been suggested to be a flexible element in the sprocket disc range as well. The composite design of the chain roller is designed to reduce the impact of the striking forces generated by the sprocket-chain coupling on the roller-bushing pair[15, 19-21].

The structure consists of a leading 1 and a driven sprocket 2 and a chain 3 covering them. The drive is equipped with a tensioning roller 4 to ensure that the mains stress is normal. The driven sprocket is made up of a toothed flange 2, a base 6, an outgoing shaft 7 and a flexible bushing 5. The chain consists of 3 inner 9 and outer 8 plates, a roller 10, a bushing 11 and a composite roller 12. The composite roller consists of 12 inner 13 and outer 14 bushings and a flexible element (rubber) 15 located between them. The flexible element 15 has a concave shape on the outer surface 16 and is made to fit the inside of the outer bushing 14.

ISSN: 2233-7857 IJFGCN

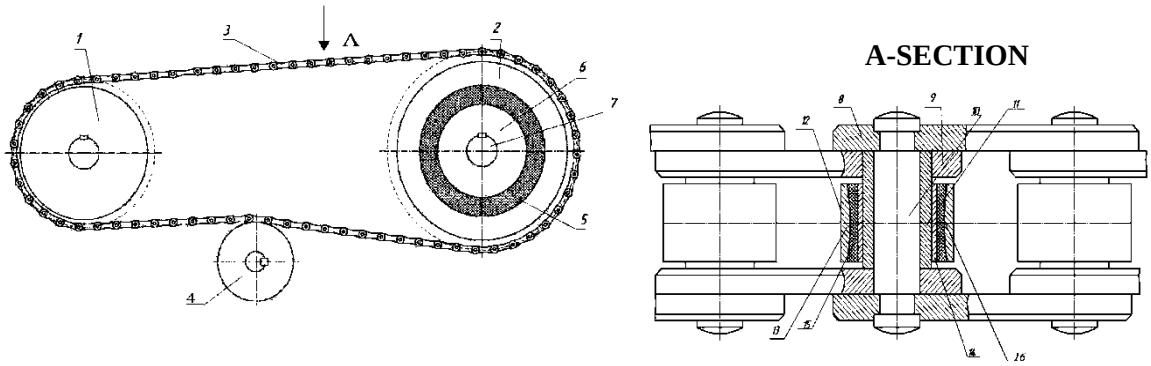

Figure 1. The scheme of chain drive with flexible element.

The proposed chain drive works in the following order: the movement from the leading sprocket 1 to the driven sprocket 2 is transmitted through the chain 3. The moving driven sprocket 2 is then transmitted to the output shaft 7 via a flexible bushing 5 and a base 6. The frictional force and other harmful forces generated between the chain 3 and the sprocket 2 are somewhat extinguished as they pass through the elastic element 5. When the chain 3 is affected by the leading 1 and the driven 2 sprockets, we can observe that the force acting on the roller-bushing pair is flat due to the deformation of the elastic element 15 in the chain roller 12. Due to the deformation of the elastic element 15, the friction between the bushing 11 and the roller 10 is also reduced. This leads to an increase in the service life of the chain drive's elements.Since the outer surface of the rubber bushing 15 has a concave appearance, an even distribution of the forces acting through the sprocket tooth is achieved. This leads to an increase in chain service life.

Static calculation of the composite roller. In performing the static calculation of the proposed chain drive roller, the roller was assumed to be in the form of a two-layer cylindrical shell (cylindrical shell) (Fig. 2).

In the static calculation of a composite roller, it is important to determine the radial displacements generated in the roller under the influence of an external load, i.e., an sprocket tooth. This is because exceeding the norm of these displacements will adversely affect the service life of the chain drive, causing the roller shaft to fail quickly. The purpose of having a composite design of the roller is to balance the impact forces and increase the service life of the rollers.

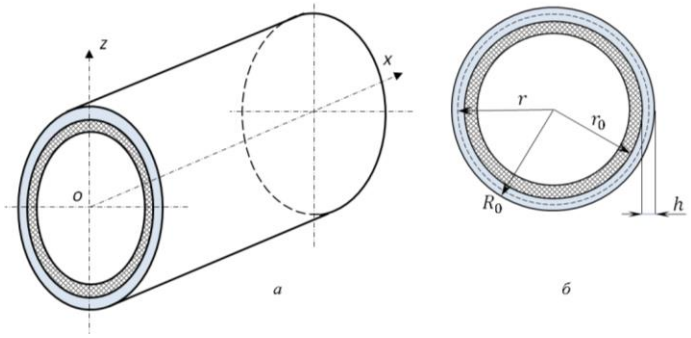

Figure 2. Composite roller calculation scheme.
a-overview of roller, b-roller cross section, r −middle surface radius, r_0 −roller inner radius, R_0 −roller outer radius, h −roller outer bushing thickness

Determination of deformation values that are symmetrical to the axis of the outer roller of the composite roller. The deformation scheme of the composite roller outer bushing is shown in Figure 3 below

ISSN: 2233-7857 IJFGCN

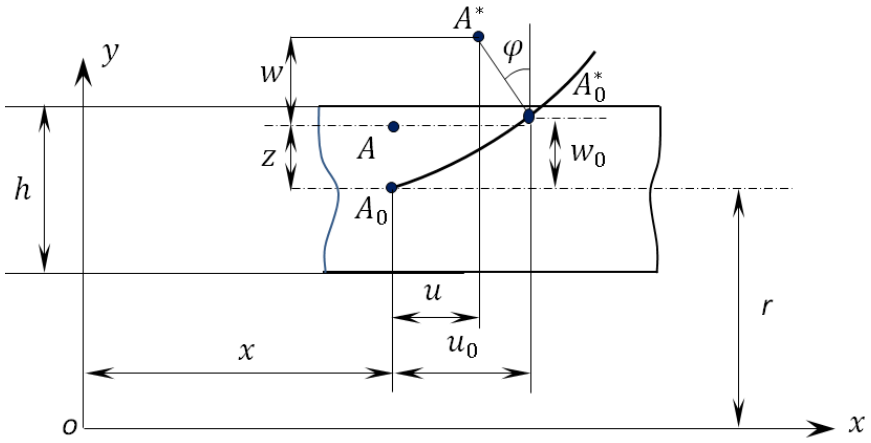

Figure 3. Deformation scheme of the outer bushing of the composite roller.

An arbitrary point in the middle section of A_0 −the outer bushing of the roller described in the calculation diagram. As a result of the deformation caused by the external load, A_0 the point moves along the axis $x$and along the radius u_0 to w_0 a quantity and occupies z the position, A_0^* while the arbitrary point A at a distance takes the position A^*: $A_0^*(u_0; w_0)$; $A^*(u; w)$.

According to the Kirchhoff-love hypothesis [22], the transition are as follows:

$$u = u_0 - z \cdot \varphi \tag{1}$$

Since the thickness of the outer bushing of the composite roller h is a small amount, we can obtain its displacement along the axis oz as follows:

$$w = w_0 \tag{2}$$

Deformations in the layer z of the composite roller are determined as follows:

$$\varepsilon_{x_0} = \frac{\partial u_0}{\partial x};\ \ \varphi = \frac{dw}{dx}. \tag{3}$$

We accept the following restrictions: $r_z = r + z \approx r$.

In this case, the deformation values (3) take the following form according to expression:

$$\begin{cases} \varepsilon_x = \varepsilon_{x_0} - z \cdot \frac{d^2w}{dx^2} \\ \varepsilon_\theta = \frac{w}{r} \end{cases} \tag{4}$$

Determination of the internal force and tension generated in the composite roller. Continuing our theoretical research, we consider the internal force and tension factors generated in a composite roller. Figure 4 shows the cross-impact power and stress acting on the longitudinal and transverse sections of the composite roller element under the influence of external loads.

Internal stresses and forces arising on the cut of the surface of the composite rollers are determined as follows:

$$\begin{cases} \sigma_x = \frac{E}{1-\mu\mu^2}(\varepsilon_x + \mu\varepsilon_\theta) \\ \sigma_\theta = \frac{E}{1-\mu^2}(\varepsilon_\theta + \mu\varepsilon_x) \end{cases} \tag{5}$$

$$\begin{cases} N_x = \frac{Eh}{1-\mu^2}(\varepsilon_{x_0} + \mu \cdot \frac{w}{r}) \\ N_\theta = \frac{Eh}{1-\mu^2}\left(\frac{\omega}{r} + \mu\varepsilon_{x_0}\right). \end{cases} \tag{6}$$

Let's enter designations: $D = \frac{Eh^3}{12(1-\mu^2)}$, where $D-$ is the roller stiffness, $\mu-$ is Poisson's ratio. As a result, we obtain the following expressions for the bending moment and relative deformations:

$$\begin{cases} M_x = D\frac{d^2w}{dx^2} \\ M_\theta = \mu D\frac{d^2w}{dx^2} \end{cases} \tag{7}$$

ISSN: 2233-7857 IJFGCN

$$\begin{cases} \varepsilon_{x_0} = \frac{du_0}{dx} = \frac{1}{Eh}(N_x - \mu N_\theta) \\ \varepsilon_{\theta_0} = \frac{w}{r} = \frac{1}{Eh}(N_\theta - \mu N_x) \end{cases} \quad (8)$$

Equations of static equilibrium of a composite roller. Based on the above internal forces, stress and relative deformations, we derive the static equilibrium equations of the composite roller. To do this, we check the balance of a small elementary part of the composite roller (Figure 5). We define the intensity q_z of the distributed compressive power acting on the middle surface of the outer roller of the composite roller by the sprocket tooth in the radial direction and the intensity of the internal elastic force (resistance).

We construct the equations of static equilibrium with respect to all the forces x and z coordinate axes acting on the elementary part of the composite roller:

$$\begin{cases} \frac{dN_x}{dx} + q_x = 0 \\ \frac{d\theta}{dx} - \frac{1}{r}N_\theta - q_z^* = 0 \end{cases} \quad (9)$$

here, as, is defined by the following expression:

$$q_z^* = q_z - kw(x) \quad (10)$$

here, q_z −the compressive force acting on the roller containing the sprocket teeth; $q_{el} = kw(x)$ −the intensity of the resistive compressive strength of the elastic element (rubber); $k -$ the coefficient of elasticity of the flexible bushing in the roller structure; $w(x) -$ radial displacement.

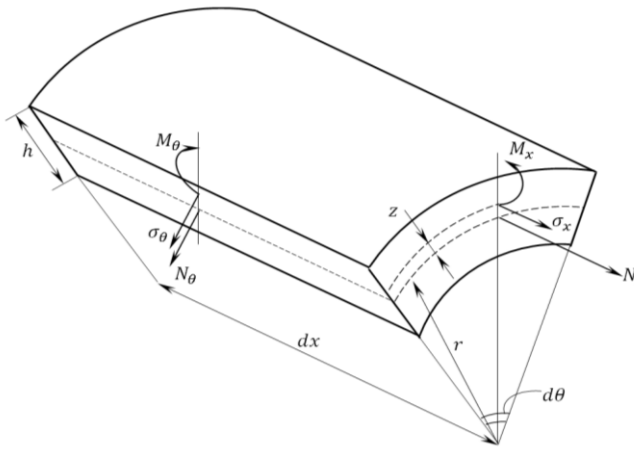

Figure 4. The power and stress acting on the lontitudinal and transverse sections of a composite roller element under the impact of an external load

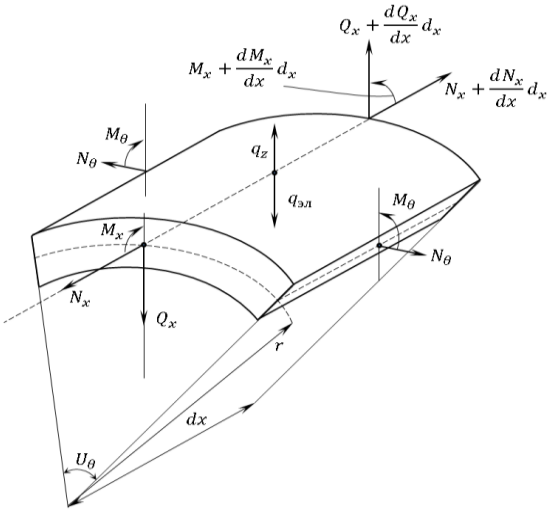

Figure 5. Cylindrical shell balancing scheme

In this case, the static equilibrium equation takes the following form.

$$\frac{d^2M_x}{dx^2} + \frac{1}{r}N_\theta = q_z^* \quad (11)$$

Substituting (6) from the expression N_θ into the expression (11), written by radial displacement $w(x)$, we obtain:

$$D\frac{d^4\omega}{dx^4} + \frac{Eh}{r^2}w(x) = q - kw(x) - \frac{M}{r}N_x \quad (12)$$

By reducing both sides of the equation to D, we obtain:

$$\frac{d^4w(x)}{dx^4} + 4\beta^4 w(x) = \frac{1}{D}q_z - \frac{M}{rD}N_x \quad (13)$$

(13) is the fourth-order differential equation that determines the transverse deformation of a roller with an expression structure.

According to expression (6), we express the longitudinal force by radial displacement, and (13) we put:

ISSN: 2233-7857 IJFGCN

$$N_x = \frac{Eh}{1-\mu^2} \cdot \mu \cdot \frac{w(x)}{r} = \left(\frac{\mu \cdot Eh}{(1-\mu^2)r}\right) w(x).$$

In this case, the appearance of expression (13) is as follows:

$$\frac{d^4w}{dx^4} + 4\beta^4 w(x) = \frac{q_z}{D} - \frac{\mu}{rD} \cdot \frac{\mu Eh}{(1-\mu^2)r} w(x) \tag{14}$$

here we enter the following definition:

$$4\beta^4 = \frac{Eh}{Dr^2}\left[1 + \frac{\mu^2}{1-\mu^2} + \frac{k \cdot r^2}{Eh}\right]$$

In that case, expression (14) takes the following form:

$$\frac{d^4w}{dx^4} + 4\beta^4 w = \frac{q_z}{D} \tag{15}$$

(15) is the equation of static equilibrium of a roller containing a differential equation.

We accept that the intensity of the compressive force acting on the composite roller through the sprocket tooth is $const$constant:$q_z = q_0 = const$.

We express the general solution of expression (15) using Krylov's fundamental functions [23-27]:

(16)

We look for a special solution as follows:

$$w(x) = A \tag{17}$$

In that case, we determine A −the value by substituting expression (17) into expression (15):

$$4\beta^4 \cdot A = \frac{q_0}{D} \text{ out of this , } A = \frac{q_0}{4D\beta^4}; w_*(x) = \frac{q_0}{4D\beta^4}. \tag{18}$$

Hence, the complete solution of expression (15) is as follows:

$$w(x) = w_1(x) + w_*(x) \text{ or}$$

$$w(x) = \mathrm{C}_1 e^{-\beta x} cos\beta x + \mathrm{C}_2 e^{-\beta x} sin\beta x + \frac{q}{4D\beta^4} \tag{19}$$

here are unknown invariables, which are determined using the following boundary conditions:

$$x = 0;\ w(0) = 0;\ w'(0) = 0 \tag{20}$$

By differentiating the expression (19) once x , we obtain the following expression:

$$w'(x) = -\mathrm{C}_1 \beta e^{-\beta x} \cdot (cos\beta + sin\beta x) + \mathrm{C}_2 \beta e^{-\beta x}(cos\beta - sin\beta x) + w'(x) \tag{21}$$

Substituting (19) and (21) into the conditions, we determine the invariable quantities:

$$w(0) = C_1 + \frac{q}{4D\beta^4} = 0 \Rightarrow\ C_1 = -\frac{q}{4D \cdot \beta^4} \tag{22}$$

$$w'(0) = -C_1\beta + C_2\beta + 0 = 0 \Rightarrow C_1 = C_2 \tag{23}$$

Hence, considering expression (19), we can write the function as follows:

$$w(x) = -C_1 e^{-\beta x}[cos\beta x + sin\beta x] + \frac{q}{4D\beta^4}$$

$$\text{Or } w(x) = \frac{q}{4D\beta^4}\left[1 - e^{-\beta x}(cos\beta x + sin\beta x)\right] \tag{24}$$

Theoretical study of dynamic vibrations under the influence of sprocket teeth of a composite roller. We create the differential equation of transverse vibrational motion of a composite roller by adding the force of inertia to the static equilibrium equations (15):

$$\frac{\partial^4 w(x,t)}{\partial x^4} + 4\beta^4 w(x,t) + \frac{\rho h}{D} \cdot \frac{\partial^2 w(x,t)}{\partial t^2} = Q_0 cospt \tag{25}$$

here, $Q_0 = \frac{P_0}{S_c \cdot D}$; $P_0 -$ external force, $S_c -$ the outer surface of the composite roller; $p -$ the oscillation frequency of the external pressure force, $D -$ cylindrical stiffness; $w = w(x,t) -$ displacement of the roller in transverse bending; $t -$time.

(25) consists of the sum of the complete solution of the differential equation, the general solution, and the special solutions.

Determining the general solution of the differential equation of dynamic vibration. We determine the solution of equation (25) without taking into account the external pressure force.

$$\frac{ph}{D} \cdot \frac{\partial^2 w}{\partial t^2} + \frac{\partial^4 w}{\partial x^4} + 4\beta^4 w = 0 \tag{26}$$

ISSN: 2233-7857 IJFGCN

This equation (26) is a homogeneous differential equation, the solution of which we seek in the following function view:

$$w(x,t) = f(t) \cdot e^{-\beta x}(cos\beta x + sin\beta x) \quad (27)$$

We apply expression (27) to expression (26). To do this, we calculate the following:

$$\frac{\partial^2 w}{\partial t^2} = f''(t) \cdot e^{-\beta x}(cos\beta x + sin\beta x); \frac{\partial^4 w}{\partial x^4} = 4\beta^4 f(t) \cdot e^{-\beta x}(cos\beta x) + sin\beta x)$$

$\frac{ph}{D} = D_*$ we apply these symbols.

Taking into consideration given the above expressions, we construct the following expression instead of (26):

$$D_* f''(t) + 8\beta^4 f(t) = 0 \quad (28)$$

If it is $k_0^2 = \frac{8\beta^4}{D_*} -$, (28) expression gains the following appearence:

$$f''(t) + k_0^2 f(t) = 0 \quad (29)$$

As a result, we obtain the differential equation of free vibration. Let the initial conditions be as follows:

$$\begin{cases} t = 0; f(0) = f_0;\ f_0 = w_0 \\ f'(0) = v_0 \end{cases} \quad (30)$$

The solution of expression (29) is as follows:

$$f_1(t) = a \cdot \sin(k_0 t + \alpha) \quad (31)$$

here , $a = \sqrt{w_0^2 + \frac{v_0^2}{k_0^2} -}$ free oscillation amplitude; $\alpha = arctg\frac{w_0 k_0}{v_0} -$ free oscillation frequency shift phase.

So the general solution looks like this:

$$w_1(x,t) = f_1(t)e^{-\beta x}(\cos\beta x + sin\beta x) \quad (32)$$

or $w_1(x,t) = a \cdot \sin(k_0 t + \alpha_0) \cdot e^{-\beta x}(cos\beta x + sin\beta x)$.

Determination of the specific solution of the differential equation of dynamic vibration. We look for a special solution of the differential equation of dynamic oscillation as follows:

$$w_2(x,t) = M \cdot cospt \cdot e^{-\beta x}(cos\beta x + sin\beta x) \quad (33)$$

Here we obtain the following expression by substituting $p -$the external pressure force oscillation frequency at (33) ⇒ (25):

$$-\frac{\rho h}{D} p^2 M + 8\beta^4 M = Q_0$$

Out of this, $M = \frac{Q_0}{8\beta^4 - \frac{\rho h}{D} \cdot p^2}$ (34)

A custom solution according to the above expressions:

$$w_2(x,t) = M \cdot cospt \cdot e^{-\beta x}(cos\beta x + sin\beta x) \quad (35)$$

The complete solution of the forced oscillating motion of the roller would be as follows:

$$w(x,t) = w_1(x,t) + w_2(x,t) \quad (36)$$

or $w(x,t) = [a \cdot sin(k_0 t + \alpha_0) + b_0 cospt] \cdot e^{-\beta x}(cos\beta x + sin\beta x)$ (37)

Here : $a = \sqrt{w_0 + \frac{v_0^2}{k_0^2}} -$ free oscillation amplitude; $k_0 = \sqrt{\frac{8\beta^4}{D}} -$ free vibration frequency; $\alpha_0 = arctg\frac{w_0 \cdot k_0}{v_0} -$ shear phase in free oscillation; $b_0 = \frac{Q_0}{8\beta^4 - \frac{\rho h}{D} p^2} -$ forced oscillation amplitude; $p -$ frequency of forced vibration motion.

The amplitude of the forced oscillation motion is calculated by the following expression:

Here, it is called static displacement and dynamic coefficient.

Using the defined analytical expressions, we set the geometric dimensions of the proposed chain drive roller (Figure 6).

ISSN: 2233-7857 IJFGCN

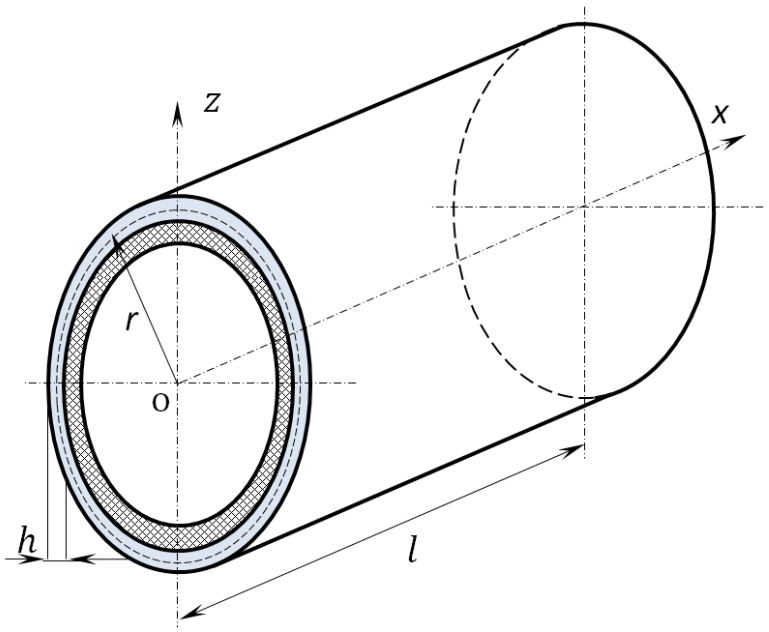

Figure 6. Geometric parameters of the composite roller

Based on the existing geometric and technological characteristics, we introduce the main quantities:

- the material of the outer bushing of the composite roller is steel, the value of the modulus of elasticity for the material: $E = 2{,}06 \cdot 10^5 MP\text{a} = 2{,}06 \cdot 10^5 \frac{N}{mm^2}$;

-the force acting on the roller with the impact component through the sprocket tooth: $P_0 = 1300\ N$;

- the length of the composite roller: $l = 14mm$;
- the thickness of the outer bushing of the composite roller: $h = 2mm$;
- Poisson's coefficient: $\mu = 0{,}3$;
- the radius of the composite roller: $r = 8mm$;
- sprocket radius: $R = 77{,}165mm$ $(D = 154{,}33mm)$;
- the angular velocity of the sprocket: $\omega_2 = 50\ s^{-1}$;
- the linear velocity of the chain $v_0 = \omega_2 \cdot R = 3858{,}25 \frac{mm}{\text{c}}$
- density of steel material: $\rho_{st} = 0{,}7850 \cdot 10^{-5}\ \frac{kg}{mm^3}$
- the surface of the roller: $S_s = 2\pi r \cdot l = 703{,}36mm^2$
- intensity of external pressure force: $Q_0 = \frac{P_0}{S_s} = 1{,}85 \frac{N}{mm^2}$;
- content roller stiffness: $D = D_1 = \frac{Eh^3}{12(1-\mu^2)} = 1{,}51 \cdot 10^5\ N \cdot mm$;

$$D_0 = \frac{Eh}{r^2} = 6437{,}5 \frac{N}{mm^3};\ d_1 = \frac{D_0}{D_1} = 0{,}043\ mm;\ D_* = \frac{\rho h}{D_1} = 1{,}04 \cdot 10^{-10} \left[\frac{s^2}{mm^4}\right]$$

$k_{oi} = \sqrt{\frac{8\beta^4}{\frac{\rho h}{D}}} -$ free oscillation motion frequency;

elastic coefficient of elastic bushing k: $\frac{k}{p} = n = 0{,}2; 0{,}3; 0{,}4; 0{,}5; 0{,}6$.

The bending moment, normal stress and relative deformations formed in the cross section of the composite roller are calculated by the following formulas:

a) torque: $M_\theta = \mu \cdot D \frac{d^2w}{dr^2}$; b) relative deformation: $\varepsilon_\theta = \frac{w}{r}$;

c) normal stress: $\sigma_\theta = \frac{E}{1-\mu^2} \cdot \varepsilon_\theta$;

ISSN: 2233-7857 IJFGCN

For static, dynamic stress cases, $k-$ transformation graphs were obtained in the MAPLE-17 program at different values of the transverse displacement, relative displacement, and shear change variables (Figures 7-14).

Result and discussion: The graph of the change in the dependence of the transverse static displacement $w(x)$ of the composite roller on the $k-$different coefficients of the elastic element along its length is given in Figure 7. When the existing chain drive roller is affected by an external load force, $P_0 = 1300\ N$ the nominal value of the transverse static displacement i.e $k = 0.$, (Fig. 7, graph 1) equals to $w = 2{,}6 \cdot 10^{-4} mm$. The nominal value of the static displacement in the value of the coefficient$k = 0{,}2$ of elasticity (Fig. 7, graph 2) $w = 2{,}3 \cdot 10^{-4} mm$, $k = 0{,}3$ (Fig. 7, graph 3) $w = 2{,}05 \cdot 10^{-4} mm$,$k = 0{,}4$, (Fig. 7, graph 4) $w = 1{,}95 \cdot 10^{-4} mm$,$k = 0{,}5$, when the force acting on the roller of the proposed composition is affected by force $P_0 = 1300\ N$ by the tooth. (Fig. 7, graph 5) $w = 1{,}88 \cdot 10^{-4} mm$, $k = 0{,}6$ (Fig. 7, graph 6) $w = 1{,}709 \cdot 10^{-4} mm$.

From the analysis of the graphs in Figure 7, it can be concluded that the transverse static displacement values decrease as the elastic coefficient of the elastic element increases. This in turn leads to a reduction in frictional forces and harmful shocks in the roller-bushing pair located under the roller.

Figure 8 shows graphs of $t-$ time-dependent change $k-$in the various coefficients of the elastic element, based on the maximum static value w_{max} of the transverse dynamic displacement $w_d(x,t)$of the composite roller along its length.

The transverse dynamic displacements of the existing chain drive roller are nominal value, i.e. $k = 0$ (Fig. 8, graph. 1) $w_d = 2{,}56 \cdot 10^{-4} mm$, maximum value $w_d = 2{,}90 \cdot 10^{-4} mm$, and amplitude value . When the elastic element in the proposed composite roller has a value of the coefficient of elasticity $k = 0{,}2$ (Fig. 8, Figure 2), the minimum value of the dynamic displacement in the composite roller is $w_d = 2{,}17 \cdot 10^{-4} mm$, the maximum value is $w_d = 2{,}44 \cdot 10^{-4} mm$, and the amplitude value is , at $k = 0{,}3$, (Fig. 8, Figure 3) the minimum value of the dynamic displacement on the content roller is $w_d = 2{,}03 \cdot 10^{-4} mm$, the maximum value is $w_d = 2{,}27 \cdot 10^{-4} mm$, the amplitude value is $w_{da} = 0{,}24 \cdot 10^{-4} mm$, at $k = 0{,}4$, the minimum value of the dynamic displacement $w_d = 1{,}89 \cdot 10^{-4} mm$ on the content roller (Fig. 8, Figure 4) $w_d = 2{,}11 \cdot 10^{-4} mm$ is the maximum value, and the amplitude value of the dynamic displacement is , at $k = 0{,}5$, $w_d = 1{,}77 \cdot 10^{-4} mm$ is the minimum value of the dynamic displacement on the roller (Fig. 8, Figure 5), and $w_d = 1{,}98 \cdot 10^{-4} mm$ is the maximum value, and at $k = 0{,}6$, $w_d = 1{,}66 \cdot 10^{-4} mm$ is the amplitude value of the dynamic displacement on the roller, $w_d = 1{,}66 \cdot 10^{-4} mm$ is the minimum value of the dynamic displacement on the composite roller (Fig. 8, Fig. 6) $w_d = 1{,}86 \cdot 10^{-4} mm$ is the maximum value of, and the amplitude value of the dynamic displacement is

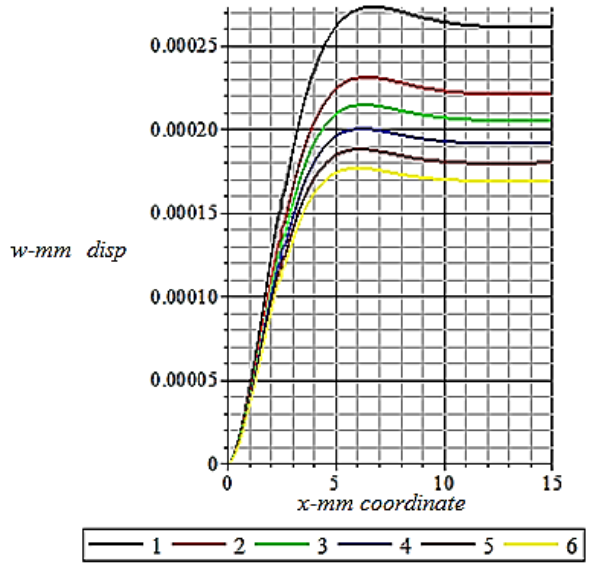

Figure 7. The change in the transverse static displacement $w(x)$ of the composite roller

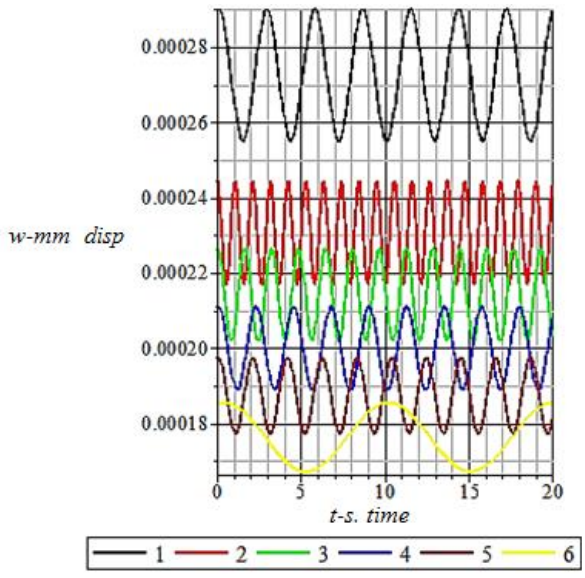

Figure 8. Based on $w_{max}$the maximum static value of the transverse dynamic displacement of

ISSN: 2233-7857 IJFGCN

depending on the $k-$ different coefficients of the elastic element along the length of the roller. Here, $1-k=0;\ 2-k=0{,}2;\ 3-k=0{,}3;\ 4-k=0{,}4;\ 5-k=0{,}5;\ 6-k=0{,}6.$

the composite roller along the length of the roller $w_d(x,t)$, $t-$ the time-dependent variation of the elastic element at k different-coefficients. Here , $1-k=0;\ 2-k=0{,}2;\ 3-k=0{,}3;\ 4-k=0{,}4;\ 5-k=0{,}5;\ 6-k=0{,}6.$

From the analysis of the graphs (Fig. 8) it can be concluded that we can observe a decrease in the values of dynamic displacement and amplitude as k the coefficient of elasticity increases. With a decrease in the dynamic displacement w_d and its amplitude value w_a, a reduction in the amount of harmful effects on the chain elements and, in turn, a slowing down of the degradation process is achieved.

Figure 9 shows the graph of the static moment generated in the cross section of a composite roller along its length, depending on k −the different coefficients of the elastic element. The value of the static moment generated in the cross section of the existing chain drive roller (Fig. 9, graph 1), static moment formed in the cross section when $k=0{,}2$ is the value of the coefficient of elasticity of the roller of the proposed composition (Fig. 9, graph 2) , at $k=0{,}3$ static moment generated in the cross section (Fig. 9, graph 3), $M_{st}=4{,}73N\cdot mm$ $k=0{,}4$ (Fig. 9, graph 4), $M_{st}=4{,}59N\cdot mm$ $k=0{,}5$ (Fig. 9, graph 5), $M_{st}=4{,}44\ N\cdot mm$ (Fig. 9, graph 6) . $M_{st}=4{,}31N\cdot mm$ $k=0{,}6.$

It can be concluded from the graph that we can observe that the static torque generated in the cross section of the roller decreases as the coefficient of elasticity of the elastic element increases. This in turn means a reduction in static impact on other elements of the chain connected to the roller.

Figure 10 shows graphs of the dynamic moment M_d generated in the cross section of a composite roller along the length of the roller, at $k-$ different coefficients of the elastic element, $t-$depending on time. From the graphs (Fig. 10.1) we can see that the dynamic moment M_d generated by the cross-sectional value $k=0$ of the existing chain drive roller under the influence of the force from the sprocket tooth $M_d=5{,}01\ N\cdot mm$ is the minimum value of the roller length, the maximum value of $M_d=5{,}69\ N\cdot mm$, and the amplitude value of $\Delta M_d=0{,}68N\cdot mm.$

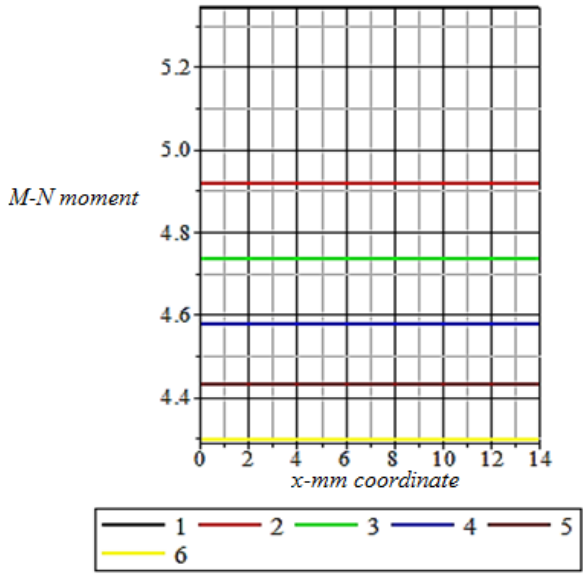

Figure 9. Static torque generated in the cross section of a composite roller along the length of the roller, the dependence of the elastic element on $k-$ different coefficients Here, $1-k=0;\ 2-k=0{,}2;\ 3-k=0{,}3;\ 4-k=0{,}4;\ 5-k=0{,}5;\ 6-k=0{,}6.$

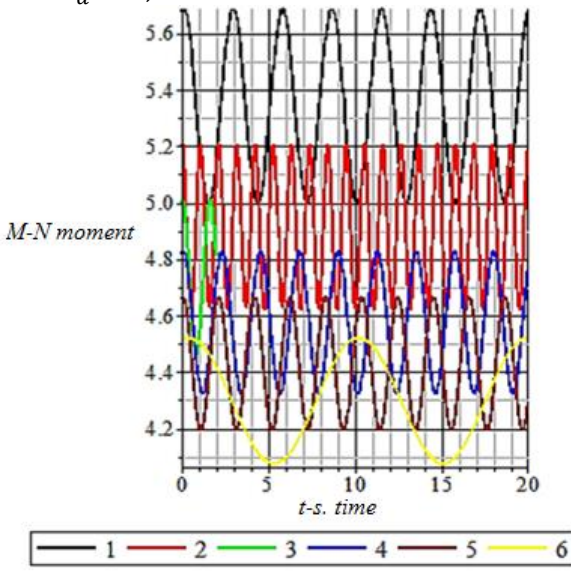

10-расм.. Figure 10. Depending on the length of the roller of the dynamic moment M_d generated in the cross section of the composite roller, the elastic element is different. in $k-$coefficients, change over $t-$time here , $1-k=0;\ 2-k=0{,}2;\ 3-k=0{,}3;\ 4-k=0{,}4;\ 5-k=0{,}5;\ 6-k=0{,}6.$

ISSN: 2233-7857 IJFGCN

Also, at the value of $k = 0{,}2$ the coefficient of elasticity of the proposed transmission roller flexible element (Fig. 10, graph 2), $M_d = 4{,}63\ N \cdot mm$ is the minimum value of the dynamic moment generated in the cross section of the roller $M_d = 5{,}21\ N \cdot mm$ is the maximum value, and the amplitude change $\Delta M_d = 0{,}58\ N \cdot mm.\ \ M_d = 4{,}47\ N \cdot mm.$ The minimum value of the dynamic moment generated in the cross section of the roller containing the value $k = 0{,}3$ (Fig. 10, graph 3). the maximum value is $M_d = 5{,}02\ N \cdot mm$, the amplitude change $\Delta M_d = 0{,}55\ N \cdot mm$, at the value of $k = 0{,}4$ (Fig. 10, graph 4), minimum value of dynamic moment is $M_d = 4{,}32\ N \cdot mm$, maximum value is $M_d = 4{,}82\ N \cdot mm$, the amplitude change $\Delta M_d = 0{,}50\ N \cdot mm$, at the value of $k = 0{,}5$ (Fig. 10, graph 5), the minimum value of the dynamic moment is $M_d = 4{,}21\ N \cdot mm$ the maximum value is $M_d = 4{,}66\ N \cdot mm$, and the amplitude change is $\Delta M_d = 0{,}45N \cdot mm$, $k = 0{,}6$ at the value of (Fig. 9, graph 6), the minimum value of the dynamic moment is $M_d = 4{,}09\ N \cdot mm$ the maximum value is $M_d = 4{,}52\ N \cdot mm$, and the amplitude change is $\Delta M_d = 0{,}43\ N \cdot mm$.

From the analysis of the graphs it can be seen that as the coefficient of elasticity of the composite roller bushing increases, the value of the dynamic moment generated in the cross section of the roller decreases. This, in turn, indicates that the flexible bushing has the property of quenching external dynamic forces.

Figure 11 shows a graph of the transverse relative deformation ε_s of a composite roller with respect to different coefficients $k$of the elastic element along its length. The value of static relative deformation (in $k = 0$) formed in the cross section of the existing chain drive roller under the influence of external load (Fig. 11 – graph 1) is $\varepsilon_s = 3{,}42 \cdot 10^{-5}$. When $k = 0{,}2$the value of the coefficient of elasticity of the roller bushing of the proposed composite roller (Fig. 11, graph 2), $\varepsilon_s = 2{,}9 \cdot 10^{-5}$ is the value of static relative deformation formed in the cross section of the roller is determined by $k = 0{,}3$ (Fig. 11.3) $\varepsilon_c = 2{,}7 \cdot 10^{-5}$, $k = 0{,}4$ (Fig. 11.4- graph) $\varepsilon_c = 2{,}5 \cdot 10^{-5}$, $k = 0{,}5$ (Fig. 11, graph 5) $\varepsilon_s = 2{,}23 \cdot 10^{-5}$, and $k = 0{,}6$ (Fig. 11, graph 6) $\varepsilon_s = 2{,}22 \cdot 10^{-5}$.

It can be concluded from the graph that we can see that the value of ε of the static relative deformation decreases with increasing coefficient of elasticity of the elastic element in the composition of the composite roller.

Figure 12 shows a graph of the transverse ε_d −dynamic relative deformation of a composite roller with respect to the $k$coefficients of elasticity of the elastic element along the length of the roller. At the maximum value $k = 0$ of the relative static deformation formed in the cross section of the existing chain drive roller under the influence of external load (Fig. 12, graph 1). $\varepsilon_d = 3{,}62 \cdot 10^{-5}$ minimum value is $\varepsilon_d = 3{,}19 \cdot 10^{-5}$, while the amplitude value is $\Delta\varepsilon_d = 0{,}43 \cdot 10^{-5}$. The maximum value of the dynamic relative deformation of the cross section of the roller when $k = 0{,}2$ the value of the coefficient of elasticity of the roller bushing of the proposed composition (Fig. 12, graph 2) is $\varepsilon_d = 3{,}05 \cdot 10^{-5}$, minimum value is $\varepsilon_d = 2{,}71 \cdot 10^{-5}$ while the amplitude value is $\Delta\varepsilon_d = 0{,}34 \cdot 10^{-5}$, at $k = 0{,}3$ (Fig. 12, graph 3) maximum value of relative deformation is $\varepsilon_d = 2{,}82 \cdot 10^{-5}$, minimum value is $\varepsilon_d = 2{,}52 \cdot 10^{-5}$ while the amplitude value is $\Delta\varepsilon_d = 0{,}30 \cdot 10^{-5}$, at $k = 0{,}4$ (Fig. 12, graph 4) maximum value of relative deformation is $\varepsilon_d = 2{,}64 \cdot 10^{-5}$, minimum value is $\varepsilon_d = 2{,}36 \cdot 10^{-5}$ while the amplitude value is $\Delta\varepsilon_d = 0{,}28 \cdot 10^{-5}$, $k = 0{,}5$ (Fig. 12, graph 5) maximum value of relative deformation is $\varepsilon_d = 2{,}47 \cdot 10^{-5}$, minimum value is $\varepsilon_d = 2{,}22 \cdot 10^{-5}$ the amplitude value is $\Delta\varepsilon_d = 0{,}25 \cdot 10^{-5}$, $k = 0{,}6$ (Fig. 12, graph 6) maximum value of relative deformation is $\varepsilon_d = 2{,}32 \cdot 10^{-5}$, minimum value is $\varepsilon_d = 2{,}19 \cdot 10^{-5}$ the amplitude value is $\Delta\varepsilon_d = 0{,}13 \cdot 10^{-5}$.

It can be concluded from the graph that ε_d the relative dynamic deformation and $\Delta\varepsilon_d$ amplitude value of the transverse dynamics of the roller decreases as the elastic coefficient of elasticity of the composite roller increases.

ISSN: 2233-7857 IJFGCN

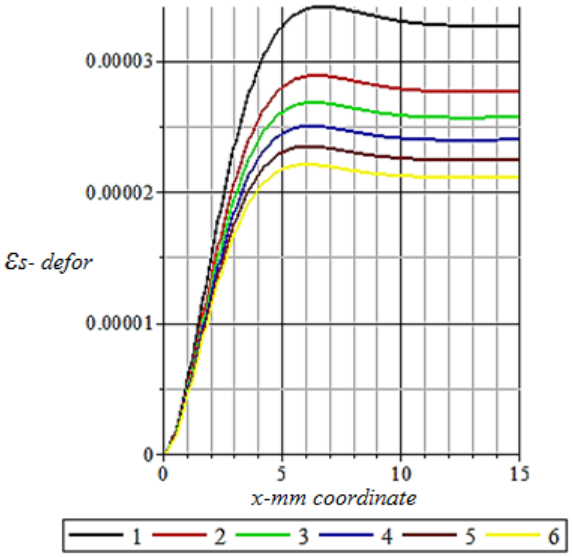

Figure 11. Variation of the transverse $\varepsilon(x)$-static relative deformation of the composite roller along the length of the roller with $k-$ different coefficients of the elastic element Here , $1-k=0;\ 2-k=0{,}2;\ 3-k=0{,}3;\ 4-k=0{,}4;\ 5-k=0{,}5;\ 6-k=0{,}6.$

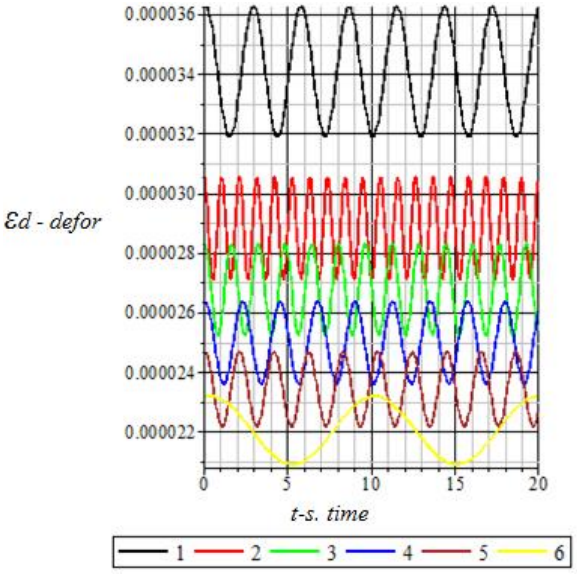

Figure 12. Variation of the transverse dynamic relative deformation $\varepsilon(x,t)$ of the composite roller depending on the k different coefficients of the elastic element along the length of the roller
Here , $1-k=0;\ 2-k=0{,}2;\ 3-k=0{,}3;\ 4-k=0{,}4;\ 5-k=0{,}5;\ 6-k=0{,}6.$

Figure 13 shows the change graphs of the static stress $\sigma(x)$generated in the cross section of the composite roller under the influence of external load depending on the k different coefficients of the elastic element along its length. Nominal value of static stress σ generated in the cross section of the existing chain drive roller under the influence of external load at $k=0$ (Fig. 13, graph 1) $\sigma=0{,}925\frac{N}{mm^2}$, the coefficient of elasticity of the roller elastic element of the proposed composition is $k=0{,}2$ static stress is σ nominal value of (Figure 13. Graph 2) $\sigma=0{,}777\frac{N}{mm^2}$, at $k=0{,}3$ (Figure 13. Graph 3) static stress $\sigma=0{,}733\frac{N}{mm^2}$, at $k=0{,}4$ (Figure 13. Graph 4) static stress $\sigma=0{,}681\frac{N}{mm^2}$, at $k=0{,}5$ (Figure 13. Graph 3) static stress $\sigma=0{,}633\frac{N}{mm^2}$, at $k=0{,}6$ (Figure 13. Graph 3) static stress $\sigma=0{,}598\frac{N}{mm^2}$.

From the graph we can see that σ the value of static stress decreases with increasing coefficient of elasticity of the elastic element in the composition of the roller.

Figure 14 shows a graph of the change in the σ_d dynamic stress generated in the cross section of a composite roller depending on the k different coefficients of elasticity of the elastic element along the length of the roller.

ISSN: 2233-7857 IJFGCN

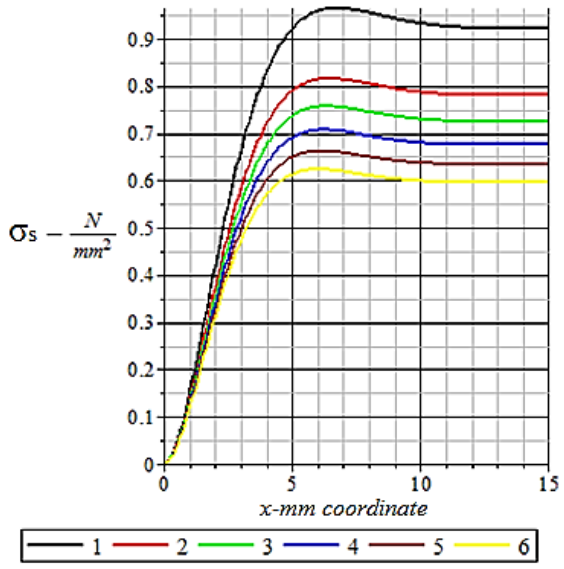

Figure 13. Variation of the transverse static stress σ(x) of the composite roller along the length of the roller depending on the k different coefficients of the elastic element
Here , $1-k=0;\ 2-k=0{,}2;\ 3-k=0{,}3;\ 4-k=0{,}4;\ 5-k=0{,}5;\ 6-k=0{,}6.$

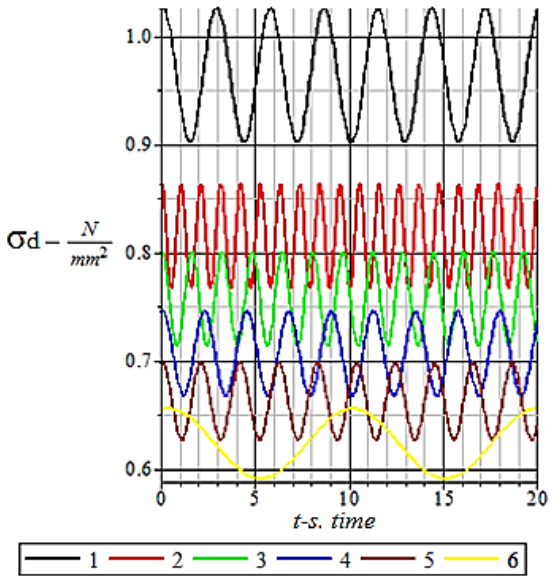

Fig. 14. The change in the transverse dynamic stress σ(x,t) of the composite roller , depending on the k –different coefficients of the elastic element along the length of the roller.
Here , $1-k=0;\ 2-k=0{,}2;\ 3-k=0{,}3;\ 4-k=0{,}4;\ 5-k=0{,}5;\ 6-k=0{,}6.$

From the graph we can see that the maximum value of the amount of stress generated in the cross section of the roller of the existing chain extension chain under the influence of external load (Fig. 14, graph 2) minimum value and amplitude value $\sigma_d = 1{,}248\frac{N}{mm^2}$, when the coefficient of elasticity of $\sigma_d = 0{,}908\frac{N}{mm^2}$ the roller elastic element $\Delta\sigma_d = 0{,}34\frac{N}{mm^2}$, of the proposed composition is $k = 0{,}2$, dynamic stress is σ_d the maximum value (Fig. 14, graph 2) $\sigma_d = 0{,}865\frac{N}{mm^2}$, minimum value $\sigma_d = 0{,}772\frac{N}{mm^2}$ and amplitude value , at the value $k = 0{,}3$ stress is σ_d the maximum value (Fig. 14, graph 3) $\sigma_d = 0{,}801\frac{N}{mm^2}$, minimum value $\sigma_d = 0{,}721\frac{N}{mm^2}$ and amplitude value $\Delta\sigma_d = 0{,}080\frac{N}{mm^2}$, at the value $k = 0{,}4$ stress is σ_d the maximum value (Fig. 14, graph 4), $\sigma_d = 0{,}749\frac{N}{mm^2}$, minimum value $\sigma_d = 0{,}674\frac{N}{mm^2}$ and amplitude value $\Delta\sigma_d = 0{,}075\frac{N}{mm^2}$, at $k = 0{,}5$ stress σ_d the maximum value (Fig. 14, graph 5), $\sigma_d = 0{,}698\frac{N}{mm^2}$ minimum value $\sigma_d = 0{,}629\frac{N}{mm^2}$ and amplitude value $\Delta\sigma_d = 0{,}069\frac{N}{mm^2}$, at the value of $k = 0{,}6$ the maximum value of stress σ_d (Fig. 14, graph 5), $\sigma_d = 0{,}651\frac{N}{mm^2}$ minimum value $\sigma_d = 0{,}589\frac{N}{mm^2}$ and amplitude value is $\Delta\sigma_d = 0{,}062\frac{N}{mm^2}$.

By analyzing the graph, we can observe an increase in the $k$coefficient of elasticity of the elastic bushing in the proposed composite roller and a decrease in the dynamic stress σ_d and $\Delta\sigma_d$ its amplitude value. It should be noted that it is possible to achieve a decrease in dynamic stress σ_d at the expense of the elastic element.

Conclusions

1. To perform a static calculation of a composite roller chain drive roller, a two-layer cylindrical shell (cylindrical shell) model of the composite roller was selected.
2. In order to check the strength and stiffness of the chain drive roller to the external compressive forces under the influence of the sprocket teeth, analytical formulas for determining the internal force factors generated in it are given.

ISSN: 2233-7857 IJFGCN

3. Using static equilibrium equations, the formulas for determining the absolute and relative deformations of the transverse deformations formed in its sections along the length of the chain drive roller are given.
4. Expressions expressing the physico-mechanical dimensions of the proposed composite roller and the coefficient of elasticity of the elastic element at different values of the deformation and internal force factors formed in the cross section were obtained and graphs of the required parameters were obtained using MAPLE-17.
5. Theoretical study of the dynamic oscillations of the composite roller under the influence of star teeth was carried out, the required graphs were obtained in MAPLE-17 program along the length of the roller, the transverse absolute and relative deformations of its sections, as well as expressions determining internal force factors.
6. Under the influence of the compressive forces of the sprocket teeth, it was found that the deformation and internal force factors generated in the chain drive roller decrease due to $7 \div 20$the presence of a flexible element.

References

1. Усова Е.В. Повышение долговечности и совершенствование технического обслуживания цепных передач сельскохозяйственного назначения. 05.20.03 – диссертация к.т.н. Зерноград: 2007.
2. Война А.А. Расчет и проектирование роликовых цепных передач с эвольвентными звездочками. 05.02.02 – диссертация к.т.н. Краснодар: 2002.
3. Бережной С.Б. Синтез и анализ роликовых цепных передач. 05.02.02-д.т.н. Краснодар: 2004.
4. Скорюнов А.А. Механика специальных роликовых цепных передач с внутренним зацеплением. 05.02.02 – диссертация к.т.н. Москва:2015.
5. Щеглов Е.В. “Совершенствование технологии обслуживания втулочно-роликовых цепей зерноуборочных комбайнов”.05.20.03 – диссертация к.т.н Москва: 2008.
6. Корнейчук Ю.А. “Повышение ресурса цепного привода распредительного вала судового малооборотного дизеля в условиях эксплуатации” 05.08.05 – диссертация к.т.н. Владивосток: 2009.
7. Семенцов М.Н. Повышение долговечности цепей сельскохозяйственных машин. 05.20.03 – диссертация к.т.н. Зерноград-2010.
8. Пашков Ю.В.“Перегрузочная способность роликовой цепной передачи” 05.02.02 – диссертация к.т.н. Краснодар:1984.
9. Стоблин Г.Б., Готовцев А.А., Проектирование цепных передач: Справочник /, И.П. Котенок. –М.: Машиностроение, 1973.-376 с.
10. А.Джураев, А.Мамахонов, Ж.Мухамедов. Цепная передача. Патент. Рес. Узб. №FAP00595, 31.12.2010, Бюл. №12, 2010г.
11. А.Джураев, А.Мамахонов, М.Умрзоқов. Цепная передача. Патент. Рес. Узб. № FAP00677., 30.12.2011, Бюл., №12.
12. А.Джураев, А.Мамахонов, М.Умирзақов. Цепная передача. Патент. Рес. Узб. № FAP00848, 31.10.2013, Бюл..,№10.
13. А.Джураев, С.Юнусов,. А.Мамахонов, Цепная передача. Патент. Рес. Узб. № FAP00919, 30.06.2014, Бюл..,№6.
14. А.Джураев, А.Мамахонов, Э.Алиев. Цепная передача. Патент. Рес. Узб. № FAP 01288, 30.03.2018, Бюл..,№3.
15. А.Джураев, А.Мамахонов, Цепная передача. Патент. Рес. Узб. №IAP05760, 28.02.2019, Бюл..,№2.

ISSN: 2233-7857 IJFGCN

16. А.Джураев, А.Мамахонов, Э.Алиев. Цепная передача. Патент. Рес. Узб. № IAP05745,31.01.2019, Бюл..,№1.
17. 19. А.Джураев, А.Мамахонов, К.Юлдашев. Цепная передача. Патент. Рес. Узб. № IAP06200, 30.04.2020, Бюл..,№4. Цепная передача.
18. A.Djurayev, A.Mamakhonov, K.Yuldashev, Improvement of the Term of Service Life of the Drive Roller Chain of Transmission. International Journal of Advanced Research in Science, Engineering and Technology. Vol. 6, Issue 3, March 2019. P.8508-8514.
19. А.Джўраев, Б.Давидбоев. А.Мамахонов Қайишқоқ элементли ва таранглаш қурилмали занжирли механизмларни кинематик ва динамик таҳлили. Монография, Монография, “Наврўз” нашриёти, “Poligraf super servis” МЧЖ босмахонаси, Тошкент-2014. 138-бет.
20. А.Джураев, А.Мамахонов, К.Юлдашев, Технологик машиналар занжирли узатмалари конструкцияларини такомиллаштириш ва параметрларини асослаш. Монография, “Фан ва технология” нашриёти, Тошкент 2019, 235-бет.
21. . Ю.В.Кириллов, А.А. Постников, А.И. Тюленев, Исследования по теории пластин и оболочек моментной теории упругости (обзор), Исслед. По теор. пластин и оболочек, 1990, выпуск 20, ст.18–43.
22. Ю.И.Виноградов, Функции коши-крылова в расчетах на прочность пластин и оболочек. Известия высших учебных заведений. Машиностроение Издательство: Московский государственный технический университет имени Н.Э. Баумана (национальный исследовательский университет) (Москва) ISSN: 0536-1044. Номер: 8 Год: 2013 Ст. 15-19.
23. И.М.Бобаков, Теория колебаний. изд-во «Наука», Москва.,1968.
24. А.С.Вольмир, Колебания пластинок и оболочек. изд-во «Наука», Москва.,1972.
25. М.А Колтуов, Т.Мавлянов, А.И.Каримов, «Об одном методе решения задачи динамической устойчивости тонкостенных вязкоупругих конструкций», Журнал “Механика композитных материалов”, Рига. №5,1980г.
26. Н.С.Пискунов, Дифференциальное уравнение и интегральное исчисление. Том 2. Изд-во «Наука», Москва.,1985 г.

ISSN: 2233-7857 IJFGCN